A Theoretical Analysis of Granulometry-Based Roughness Measures on Cartosat DEMs

Kannan Nagajothi, *Member, IEEE*, Sravan Danda, Aditya Challa, and B. S. Daya Sagar, *Senior Member, IEEE*

***Abstract*—The study of water bodies such as rivers is an important problem in the remote sensing community. A meaningful set of quantitative features reflecting the geophysical properties help us better understand the formation and evolution of rivers. Typically, river sub-basins are analyzed using Cartosat Digital Elevation Models (DEMs), obtained at regular time epochs. One of the useful geophysical features of a river sub-basin is that of a roughness measure on DEMs. However, to the best of our knowledge, there is not much literature available on theoretical analysis of roughness measures. In this article, we revisit the roughness measure on DEM data adapted from multiscale granulometries in mathematical morphology, namely *multiscale directional granulometric index (MDGI)*. This measure was classically used to obtain shape-size analysis in grayscale images. In earlier works, MDGIs were introduced to capture the characteristic surficial roughness of a river sub-basin along specific directions. Also, MDGIs can be efficiently computed and are known to be useful features for classification of river sub-basins. In this article, we ask the question *when does a MDGI fail to classify distinct DEMs?* We provide a theoretical analysis of a MDGI to answer this question. In particular, we identify nonrivial sufficient conditions on the structure of DEMs under which MDGIs cannot distinguish between distinct DEMs. These properties are illustrated with some fictitious DEMs. We also provide connections to a discrete derivative of volume of a DEM. Based on these connections, we provide intuition as to why a MDGI is considered a roughness measure. We empirically verify that MGDIs capture the topographical characteristics using the Lower-Indus, Wardha, and Barmer river sub-basins. We show that a simple decision tree based on MDGI features alone can successfully distinguish between sub-basins with a high accuracy. We obtain upto 94% accuracy while the baseline of random classifier is around 33.34%.**

***Index Terms*—Cartosat, digital elevation model (DEM), granulometric index, mathematical morphology.**

Manuscript received July 16, 2021; revised February 19, 2022; accepted March 18, 2022. Date of publication March 23, 2022; date of current version April 20, 2022. The work of Sravan Danda was supported by the BPGC/RIG/2020-21/11-2020/01 (Research Initiation Grant), GOA/ACG/2021-22/Nov/05 (Additional Competitive Grant) both provided by BITS-Pilani K K Birla Goa Campus and thank APPCAIR, and Computer Science and Information Systems, BITS-Pilani Goa. The work of B. S. Daya Sagar was supported by the DST-ITPAR-Phase-IV project under Grant INT/Italy/ITPAR-IV/Telecommunication/2018. *(Corresponding author: Sravan Danda.)*

Kannan Nagajothi is with the Regional Remote Sensing Centre, Indian Space Research Organisation, Bangalore 560037, India (e-mail: nagajothik@gmail.com).

Sravan Danda and Aditya Challa are with the Computer Science and Information Systems, APPCAIR, BITS-Pilani Goa Campus, Zuari Nagar 403726, India (e-mail: sravan8809@gmail.com; aditya.challa.20@gmail.com).

B. S. Daya Sagar is with the Systems Science and Informatics Unit, Indian Statistical Institute Bangalore Centre, Bangalore 560059, India (e-mail: bsdsagar@yahoo.co.uk).

Digital Object Identifier 10.1109/JSTARS.2022.3161667

I. Introduction

THE study of geophysical properties of rivers is an important problem in the remote sensing community [7], [8], [20], [21], [27], [29]. A study of a river sub-basin at regular time epochs over a large span of time helps understand the evolution of the river. The evolution of river sub-basins provides information required to prioritize the rivers that need immediate attention for conservation/identify natural calamities, etc. However, such a study is highly dependent on extracting meaningful geophysical features of the river sub-basins. For example, the complexity of the surficial roughness of a river sub-basin provides information as to what the dominant wind directions are, in that region. Recall that Cartosat Digital Elevation Models (DEMs) are typically used to compute geophysical features of river sub-basins. In literature, several studies indicate that surficial roughness measured on DEMs is an important characteristic of a river sub-basin and other landforms [1]–[3], [4], [5], [13], [16]–[19], [22]–[25]. For example, roughness can be used for upscaling hydraulic conductivity [14], when used as a function of age helps delimit landslides of different time epochs [11], and parametrize hydrological models for channel flow [10], etc. Effectively, roughness measures have a strong correlation with the natural processes acting on a landform. Hence, theoretical analyses on roughness can provide a better understanding of the evolution of natural processes on a landform. However, existing studies lack a detailed theoretical analysis of the roughness measures proposed. In this article, we analyze in detail, a surficial roughness measure that was proposed in [13] i.e., *multiscale directional granulometric index (MDGI)*, a special case of a more general measure namely a *multiscale granulometric index*. Multiscale granulometric index was originally proposed in [9] to obtain a shape-size analysis of objects in greyscale images. As grayscale images can be viewed as digital surfaces with the grayscale intensity at each pixel representing the height of the surface, these measures have been adapted to DEMs [24]. It was shown experimentally that such an adaptation is indeed useful from an application point-of-view, i.e., to classify river sub-basins [13]. A natural question would then be to ask: *When does a MDGI fail to classify distinct DEMs?* Equivalently, *can we characterize the equivalence classes of DEMs obtained by the relation—two DEMs are equivalent if their MDGI are identical?* In other words, can we find necessary and sufficient conditions on the structure of a DEM under which a MDGI is invariant? In this article, we partially answer this question and provide

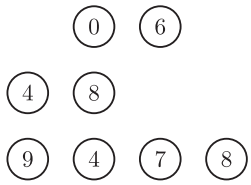

Fig. 1. Nonrectangular fictitious DEM. Each circle represents a physical square area. The values inside each of the circles are the elevations.

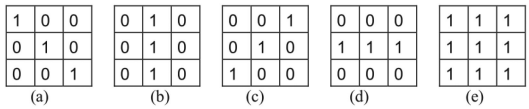

Fig. 2. *Left to right*: Types of structuring elements used in this article. The centre element refers to (0,0). A value of 1 indicates that the point corresponding to the coordinates are present in the structuring element and a value of 0 otherwise.

theoretical insights on how a MDGI varies with the structure of a DEM. In particular, the contributions of this article are as follows.

1) We provide an alternate visualization of the definition of a MDGI proposed in [13].
2) Using the alternate visualization, we characterize nontrivial sufficient conditions on DEMs under which a MDGI is invariant. The invariance properties are intuitively explained and illustrated on fictitious DEMs.
3) We analyze the relation between a MDGI and a discrete derivative of volume of a DEM. Using this analysis, we provide an intuition as to why a MDGI is considered a roughness measure.
4) We empirically verify that MGDIs capture the topographical characteristics using the Lower-Indus, Wardha, and Barmer river sub-basins. We show that a simple decision tree based on with MDGI features alone can successfully distinguish between sub-basins upto 94% accuracy while the baseline of random classifier is around 33.34%.

The rest of the article is organized as follows: In Section II, we provide the definitions of basic morphological operators and multiscale granulometric index. Also, the existing literature on the usage of directional granulometric indices is briefly described. Section III contains the core contributions of the article, i.e., an alternate visualization of a MDGI, the invariance properties, relation to discrete derivative on the volume of a DEM, and an intuition as to why a MDGI is considered a roughness measure. Section IV contains experiments on real data, i.e., on watersheds of Indus, Wardha, and Barmer river sub-basins.

II. Multiscale Granulometric Index

In this section, we recall the formal definitions of a multiscale granulometric index and briefly describe the existing literature. First, we start with the basic definitions.

A. Elementary Morphological Operators

Definition 1: Let $A \subset \mathbb{Z}^2$ be a finite set. A DEM of a river basin/sub-basin is represented as a function $f : A \to H$, where $H \subset \mathbb{Z}^+$ is a finite set.

Each point $a \in A$ represents a small physical, square area, and $f(a)$ represents the discretized average height of the physical area. Also, observe that A is possibly nonrectangular, i.e., $A = \cup_{i=n_1}^{n_2} A_i$, where $A_i = \{(i,j) : m_{1,i} \leq j \leq m_{2,i}\}$). See Fig. 1 for an illustration. This is in contrast to grayscale images, where A is always rectangular, i.e., $m_{1,i}$ and $m_{2,i}$ are independent of i. The number of distinct elements in H is comparable to the number of gray levels in a grayscale image. A higher cardinality of H indicates a finer resolution in the elevations and is analogous to a finer spectral resolution in greyscale images.

Next, we need the definition of a structuring element. Using the notion of a structuring element, dilation, and erosion, the fundamental blocks of roughness measures based on multiscale granulometric index are then defined. Note that we restrict the definition of structuring element, i.e., assume that the structuring element contains its origin and is symmetric. This definition suffices for the purposes of this article.

Definition 2: A structuring element SE $\subset \mathbb{Z}^2$ is a finite set such that: 1) $(0,0) \in$ SE, 2) $(i,j) \in$ SE $\Rightarrow (-i,-j) \in$ SE.

The different types of structuring elements used in this article are given by $B_1 = \{(-1,1),(0,0),(1,-1)\}$, $B_2 = \{(0,1),(0,0),(0,-1)\}$, $B_3 = \{(-1,-1),(0,0),(1,1)\}$, $B_4 = \{(-1,0),(0,0),(1,0)\}$, and $B = \{(x,y) \in \mathbb{Z}^2 : -1 \leq x,y \leq 1\}$. Fig. 2 provides a pictorial representation of these structuring elements. Observe that each of the structuring elements B_1, B_2, B_3, B_4 are 3 units long and are effectively one-dimensional (1-D).

Recall that a grayscale dilation and a grayscale erosion are defined as follows:

Definition 3: Let $f : A \to H$ be a DEM and let SE be a structuring element, then a dilation of f by SE is given by

$$[f \oplus \text{SE}](x,y) = \max_{(s,t)\in \text{SE}} \{f(x+s, y+t)\} \tag{1}$$

where SE is a structuring element

Definition 4: Let $f : A \to H$ be a DEM and let SE be a structuring element, then an erosion of f by SE is given by

$$[f \ominus \text{SE}](x,y) = \min_{(s,t)\in \text{SE}} \{f(x+s, y+t)\} \tag{2}$$

where SE is a structuring element

Next, we need the definition of a morphological opening and a multiscale morphological opening.

Definition 5: Let $f : A \to H$ be a DEM and let SE be a structuring element, then an opening of f is given by

$$[f \circ \text{SE}](x,y) = [[f \ominus \text{SE}] \oplus \text{SE}](x,y). \tag{3}$$

Definition 6: Let $f : A \to H$ be a DEM and let SE be a structuring element, then a multiscale opening of f is given by

$$[f \circ n\text{SE}](x,y) \tag{4}$$

where nSE $=$ SE $\oplus$ SE $\oplus \cdots \oplus$ SE with the number of dilations in the telescoping expression being $n-1$.

B. Directional Multiscale Granulometric Index

Before we provide a formal definition of a multiscale granulometric index, we need to define the notion of volume of a DEM.

Definition 7: Let $f : A \to H$ be a DEM. The volume of f, $V(f)$ is defined as follows:

$$V(f) = \sum_{a \in A} f(a). \tag{5}$$

Intuitively, the volume of a DEM captures the physical volume of a DEM on and above the altitude chosen to be zero. For example, the volume of DEM shown in Fig. 1 is 46. It is easy to see that an application of a multiscale opening results in a DEM with lower volume as n increases. Also, it is easy to see that there exists $N_0 \in \mathbb{N}$ such that $V(f \circ n\text{SE}) = V(f \circ (n+1)\text{SE})\ \forall n \geq N_0$. Recall that the definition of multiscale granulometric index is given by

Definition 8:

$$\text{GI}_{\text{SE}}(f) = -\sum_{n=0}^{\infty} p_n \log(p_n) \tag{6}$$

where

$$p_n = \frac{V(f \circ n\text{SE}) - V(f \circ (n+1)\text{SE})}{V(f)}. \tag{7}$$

Note that the existence of $N_0 \in \mathbb{N}$ such that $V(f \circ n\text{SE}) = V(f \circ (n+1)\text{SE})\ \forall n \geq N_0$ ensures that the summation is finite. The terms inside the summation for $n \geq N_0$ have to be interpreted as zero. When the structuring element SE is chosen to be one of B_1, B_2, B_3, B_4, the obtained multiscale granulometric index is said to be a directional multiscale granulometric index or MDGI. Intuitively, this makes sense as each of B_1, B_2, B_3, B_4 are linear and indicate four primary directions.

C. Existing Literature

Multiscale granulometric index was first introduced in [9] to perform a shape-size analysis of objects in grayscale images. Then, it was used to analyze textures in grayscale images [15]. Later, these ideas were generalized to analyze soil section image analysis [26]. Multiscale granulometric index was theoretically analyzed from the perspective of identifying shapes and sizes of objects in grayscale images. The utility of granulometries in grayscale images led to the development of efficient algorithms for specialized classes of structuring elements [12], [28].

Very recently, these ideas were adapted to DEMs. It was experimentally shown in [13] that multiscale granulometric indices obtained using specific structuring elements retain characteristic information of the river basins. A natural question would then be to ask: *Can we find necessary and sufficient conditions on the structure of a DEM under which the directional granulometric index is invariant?* In the next section, we partially answer this question by identifying nontrivial sufficient conditions on DEMs such that all DEMs satisfying such conditions have the same directional granulometric index.

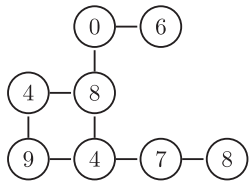

Fig. 3. Node-weighted graph constructed on the DEM given by Fig. 1. A 4-adjacency relation is used to construct the set of edges.

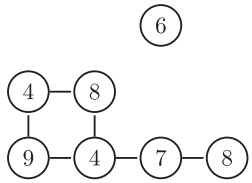

Fig. 4. Upper-thresholded graph constructed on the node-weighted graph given by Fig. 3. The threshold is set at elevation 3.

III. Theoretical Analysis of Directional Granulometric Indices

In this section, we analyze the MDGIs from a theoretical perspective. First, we recall some modified definitions from graph theory to suit the purposes of subsequent analysis on a MDGI. Second, we provide an alternate way to view a MDGI using graphs. Then, by building on this visualization of MDGI, we provide intuition on sufficient conditions under which DEMs have the MDGI. Then, we prove the main result of this article formalizing the intuition, i.e., characterization of nontrivial sufficient conditions on structure of a DEM such that the MDGI is invariant. This is followed by a short subsection analyzing the relation between MDGI and a discrete derivative of volume of a DEM. Using this analysis, we provide intuition as to why a MDGI is considered a roughness measure.

A. Some Modified Graph Definitions

Definition 9: $\mathcal{G} = (V, E, W)$ is said to be a node-weighted graph if V denotes the set of nodes is a finite set, $E \subset \{\{v_i, v_j\} : v_i \neq v_j,\ v_i, v_j \in V\}$ denotes the set of edges, and $W : V \to H$ is a non-negative integer-valued function on V such that $H \subset \mathbb{Z}^+$ is a finite set.

A node-weighted graph can be used to model DEMs taking into account the spatial relations of neighboring physical areas on which the elevations are stored. For example, Fig. 3 shows a node-weighted graph constructed on a fictitious DEM illustrated by Fig. 1.

Definition 10: Let $\mathcal{G} = (V, E, W)$ be a node-weighted graph. Let $W : V \to H$ and $h \in H$. $\mathcal{G}_{\geq h} = (V_{\geq h}, E_{\geq h}, W|_{V_{\geq h}})$ is said to be an upper-thresholded subgraph of $\mathcal{G} = (V, E, W)$ at elevation h, where $V_{\geq h} = \{v \in V : W(v) \geq h\}$, $E_{\geq h} = \{\{v_i, v_j\} : \{v_i, v_j\} \in E \text{ and } W(v_i) \geq h, W(v_j) \geq h\}$, and $W|_{V_{\geq h}}$ denotes the restriction of the function W to $V_{\geq h}$

Intuitively, an upper-thresholded subgraph of a node-weighted graph constructed on a DEM provides an abstraction of the substructure of the the DEM that is above an elevation level.

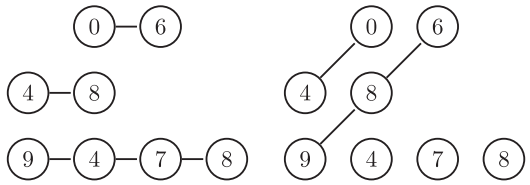

Fig. 5. 1-D scans on the DEM in Fig. 1 required to obtain a theoretical analysis of $GI_{B_4}(f)$ and $GI_{B_3}(f)$.

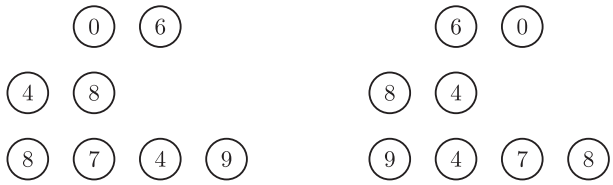

Fig. 6. Two DEMs different from the DEM provided by Fig. 1 with the same MDGI $GI_{B_4}(.)$.

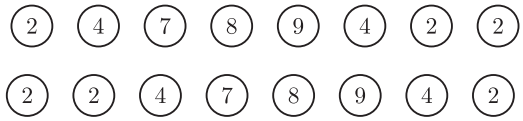

Fig. 7. Top row corresponds to one DEM and the second row corresponds to another DEM. These DEMs have identical $GI_{B_4}(.)$ but they cannot be constructed from each other using the construction provided by (14).

For example, Fig. 4 illustrates the upper-thresholded subgraph at elevation 3 on the node-weighted graph given by Fig. 3.

Definition 11: Let $\mathcal{G} = (V, E, W)$ be a node-weighted graph. A subset of nodes $V_1 \subset V$ is said to be connected if for every pair of nodes $v_s, v_t \in V_1$, there exists a sequence of nodes $< v_s = v_0, v_1, \ldots, v_{r-1}, v_r = v_t >$ such that $\{v_i, v_{i+1}\} \in E$ for every $0 \leq i \leq r-1$. A subset of nodes $V_1 \subset V$ is said to be maximally connected if 1) V_1 is connected, and 2) $V_1 \subset V_2 \subset V$ and V_2 is connected implies $V_2 = V_1$.

We remark that given any node-weighted graph $\mathcal{G} = (V, E, W)$, the set V can be decomposed uniquely as a disjoint union of maximally connected subsets of V. For example, the node-weighted graph in Fig. 3 has one maximally connected subset, which is the vertex set itself. Similarly, the upper-thresholded graph in Fig. 4, which is also a node-weighted graph has two maximally connected subsets of the vertex set.

B. Another Interpretation of a Directional Granulometric Index

Recall from Section II-B that a multiscale granulometric index is given by Def. 8 [see (6) and (7)]. Intuitively, a multiscale granulometric index measures the entropy of the volume loss on the series of morphological openings with increasing sizes of the structuring element.

Assume that the structuring element SE is given by one of B_1, B_2, B_3, B_4 as defined in Section II-A. Each of the four structuring elements are effectively 1-D. Hence, a directional granulometric index effectively measures volume loss on linear scans (but in different directions). Fig. 5 shows an illustration of the scans obtained for SEs B_4 and B_3.

Thus, same theoretical analysis on MDGI holds for each of B_1, B_2, B_3, B_4. Let $f : A \to H$ be a DEM. In order to understand the directional granulometric index better, we first try to analyze a 1-D DEM, i.e., working with DEMs restricting the domain to horizontal scans. The analysis for a generic 2-D set A would be a straightforward extension with slightly involved notation. Mathematically, such a restriction would be equivalent to working with sets of type

$$A_{i_0} = \{(i_0, j) : m_1 \leq j \leq m_2\} \subset A \tag{8}$$

for a fixed $i_0 \in \mathbb{Z}$ and $m_1 < m_2 \in \mathbb{Z}$. In general, m_1, m_2 depend on i_0 as A is not necessarily rectangular. However, we blur this detail to work with a simplified notation.

We now analyze a MDGI obtained by multiscale openings using horizontal linear structuring elements $\{L_n : n \in \mathbb{Z}^+\}$, where L_n denotes a horizontal structuring element with n consecutive 1 s. A similar analysis holds for $\{nB_4 : n \in \mathbb{Z}^+\}$ because $\{nB_4 : n \in \mathbb{Z}^+\} \subsetneq \{L_n : n \in \mathbb{Z}^+\}$ (in particular $nB_4 = L_{2n+1}$ for each $n \in \mathbb{Z}^+$). We are now ready to examine $GI_{L_1}(f|_{A_{i_0}})$ given by (6) and (7), where $f : A \to H$ is a DEM. Let $\mathcal{G}^f = (A_{i_0}, E_{\text{chain}}, f|_{A_{i_0}})$ denote a node-weighted graph with

$$E_{\text{chain}} = \{\{(i_0, j), (i_0, j+1)\} : m_1 \leq j \leq m_2 - 1\}. \tag{9}$$

Consider the sequence of upper-thresholded subgraphs of the node-weighted graph $\mathcal{G}^f = (A_{i_0}, E_{\text{chain}}, f|_{A_{i_0}})$ at all possible elevations i.e.,

$$\{\mathcal{G}^f_{\geq h}\}_{h=\min(H)}^{\max(H)} = \{(V^f_{\geq h}, E^f_{\geq h}, f|_{V^f_{\geq h}})\}_{h=\min(H)}^{\max(H)}. \tag{10}$$

Let $V^f_{\geq h} = \cup_{r=1}^{n_h} V^{f,r}_{\geq h}$ denote the disjoint union of maximally connected subsets for each $h \in [\min(H), \max(H)]$. Denote $n_{t,h}$ as

$$n_{t,h} = |\{V^{f,r}_{\geq h} : |V^{f,r}_{\geq h}| = t\}|. \tag{11}$$

Here $n_{t,h}$ denotes the number of maximally connected subsets of $V^f_{\geq h}$, which are exactly t units long. It is easy to see that the probabilities given by (7) satisfy

$$p_k \alpha \sum_{h=\min(H)}^{\max(H)} n_{k,h} \tag{12}$$

for each $k \in \mathbb{Z}^+$. This is because $L_k = kL_1$ is k units long for each $k \in \mathbb{Z}^+$. An opening with kL_1 removes any maximally connected subset of length less than k units. Hence, probability p_k is proportional to the volume obtained by slices of rectangular blocks that are k units long on the DEM f.

We are now ready to extend these ideas to a generic 2-D set A. In the 2-D case $n_{t,h}$ for each horizontal scan given by (11) would be dependent on i_0, i.e., the choice of row, denoted by $n^{(i)}_{t,h}$. Assuming $f : A \to H$ is the DEM on which we wish to compute the MDGI, (12) would transform to

$$p_k \propto \sum_{i=n_1}^{n_2} k \sum_{h=\min(H)}^{\max(H)} n^{(i)}_{k,h}. \tag{13}$$

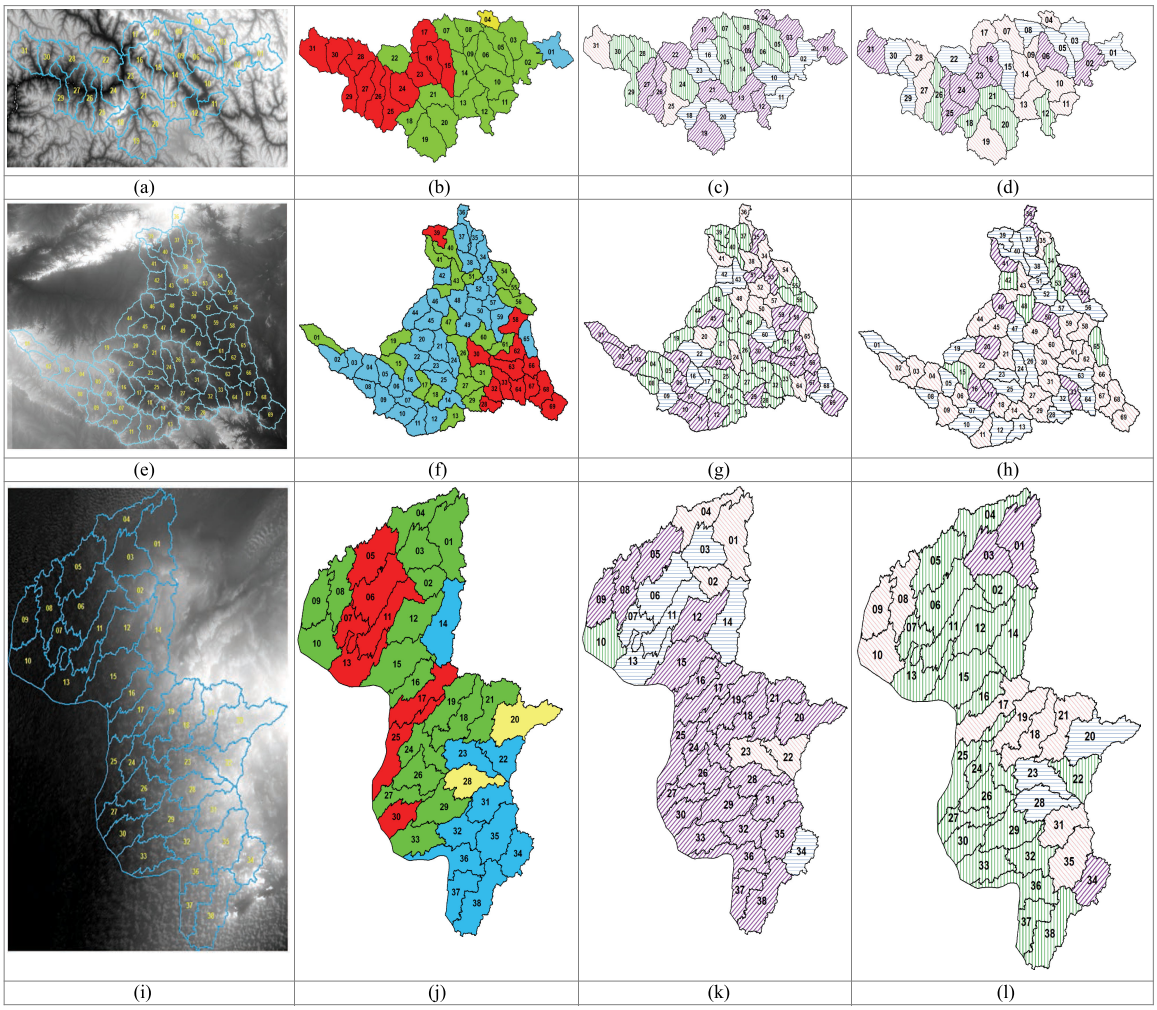

Fig. 8. (a), (e), and (i) Cartosat DEMs of Lower Indus, Wardha, and Barmer sub-basins. The delineations highlight distinct watersheds within each of the sub-basins. (b), (f), and (j) Watersheds classified based on normalized multiscale directional granulometric indices. The MDGIs are all scaled down within each sub-basin and are color-coded as per the ranges: $0-0.25$: yellow, $0.26-0.5$: blue, $0.51-0.75$: green, $0.76-1.0$: red. The ranges are arbitrarily chosen. (c), (g), and (k) high directional granulometric indices with the colors and the texture highlighting the corresponding SE for which the MDGI is highest, and (d), (h), and (l) low directional granulometric indices with the colors and the texture highlighting the corresponding SE for which the MDGI is lowest, of 31 watersheds of the Lower Indus, 69 watersheds of Wardha and 38 watersheds of Barmer sub-basins, respectively.

C. Invariances of Directional Granulometric Indices

Recall from Section II that a multiscale granulometric index is given by Def 8 [see (6) and (7)]. We are interested to characterize sufficient conditions on the structure of a DEM such that all DEMs that satisfy those conditions have the same MDGI. Mathematically, we need to find nontrivial collections of DEMs $\mathcal{F}_c = \{f | GI_{B_4}(f) = c\}$, where $c > 0$ is a positive constant. A sufficient condition for a MDGI to be invariant is that the probabilities given by (7) remain the same. On a closer look at (12), it is easy to see that if $n_{t,h}$ given by (11) remains constant for each t, h then the MDGI for each such DEM is the same. We now state the result formally:

Theorem 1: Let $f_1 : A \to H$ and $f_2 : A \to H$ be distinct DEMs. If the number of maximally connected subsets $n_{t,h}^{(i)}$ [given by (11)] of upper-thresholded subgraphs [given by (10)] for every row i, every length t, and every elevation h are identical for both f_1 and f_2 then $GI_{L_1}(f_1) = GI_{L_1}(f_2)$.

The proof follows from (13), (6), and (7). To see that the sufficient conditions imposed in Theorem 1 are nontrivial, consider $f : A \to H$. We will now construct a "large" collection of DEMs different from f whose MDGI w.r.t. B_4 is identical to that of f. Let $A = \cup_{i=n_1}^{n_2} A_i$, where $A_i = \{(i,j) : m_{1,i} \leq j \leq m_{2,i}\}$. Define $\hat{f}_i : A_i \to H$ as

$$\hat{f}_i(i,j) = f(i, m_{2,i} - j + m_{1,i}) \tag{14}$$

for each $m_{1,i} \leq j \leq m_{2,i}$. Intuitively, $\hat{f}_i$ is the mirror-reflection of $f|_{A_i}$. Now, consider the collection $\mathcal{F}_{\text{Reflection}}(f) = \{g : A \to H : g|_{A_i} = f|_{A_i} \text{ or } \hat{f}_i\}$. It is easy to see that $|\mathcal{F}_{\text{Reflection}}(f)| = 2^{n_2 - n_1 + 1}$. One of the elements of $\mathcal{F}_{\text{Reflection}}(f)$ is f. Hence, we could construct $2^{n_2-n_1+1} - 1$ different DEMs with the same MDGI. Fig. 6 provides an illustration of this construction, i.e., two DEMs different from the DEM provided by Fig. 1 with same MDGI $\text{GI}_{B_4}(.)$.

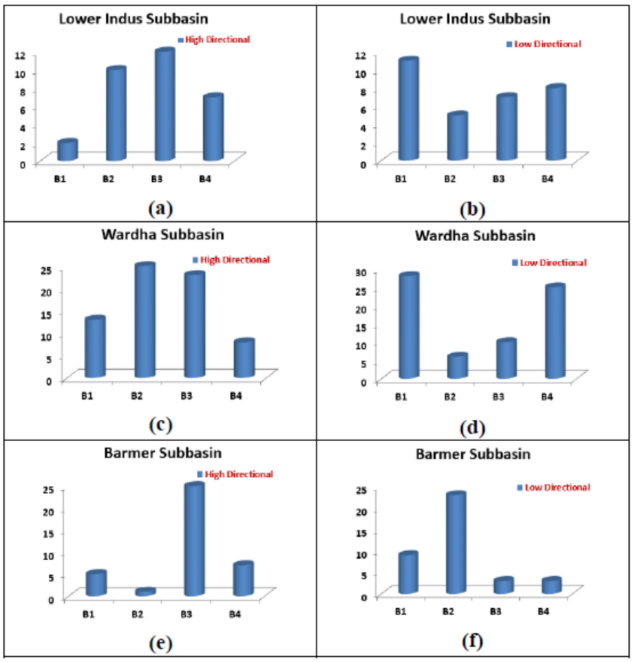

Fig. 9. (a), (c), and (e): The histograms of the highest order-statistic among normalized HDGIs obtained with B_1, B_2, B_3, B_4 as the structuring elements on Lower-Indus, Wardha, and Barmer sub-basins, respectively. (b), (d), and (f): The histograms of the lowest order-statistic among normalized HDGIs obtained with B_1, B_2, B_3, B_4 as the structuring elements on Lower-Indus, Wardha, and Barmer sub-basins, respectively.

In general, it is possible to construct much larger set of DEMs with same MDGI. This is because the domain of DEMs are usually different, i.e., arbitrary shaped DEMs are encountered in practice. Also, the conditions characterized by (14) are relatively more restrictive sufficient conditions compared to the sufficient conditions provided by Theorem 1. For example, among the DEMs illustrated in Fig. 7, one DEM cannot be constructed from the other using the construction provided by (14). However, both these DEMs have identical $n_{t,h}$ for each t, h and hence have the same MDGI $GI_{B_4}(.)$. Further, the conditions provided by Theorem 1 are sufficient but not necessary.

Next, we discuss another type of invariance, which involves transformations on the elevation level, i.e., comparing DEMs $f_1 : A \to H_1$ and $f_2 : A \to H_2$, where H_1 and H_2 are finite subsets of $\mathbb{Z}^+$. Formally, we have the following result:

Theorem 2: Let $A \subset \mathbb{Z}^+$ and $H \subset \mathbb{Z}^+$ be finite sets. Assume that $T : H \to \mathbb{Z}^+$ is a scaling transformation, i.e., $T(x) = kx$ for some arbitrary but fixed $k \in \mathbb{Z}^+$. The DEMs $f : A \to H$ and $(T \cdot f) : A \to T(H)$ have identical MDGIs, i.e., $GI_{B_l}(f) = GI_{B_l}(T \cdot f)$ for each $1 \leq l \leq 4$. Here $\cdot$ denotes composition of functions.

The proof of Theorem 2 follows from the fact that each of the terms on right side of (13) is scaled up by the same constant and hence has no effect on the LHS of the same equation.

D. Relation to Discrete Derivative of Volume of a DEM

In this section, we relate a discrete derivative of the volume of a DEM to the MDGI. First, for the sake of simplified notation, assume that we are working on horizontal slices A_i of the domain A of the DEM $f : A \to H$, i.e., subsets of the type (8) of A. Define

$$\Phi_{h_0}(f|_{A_i}) = \sum_{h=h_0}^{\max(H)} \sum_{v \in V^{f,r}_{\geq h} \subset V^f_{\geq h}} W(v). \tag{15}$$

The quantity $\Phi_{h_0}(f|_{A_i})$ denotes the volume of DEM f on and above elevation h_0 on the horizontal slice A_i. In particular, $\sum_{i=n_1}^{n_2} \Phi_{\min(H)}(f|_{A_i})$ denotes the total volume of DEM f, $V(f)$ given by (5). $\Phi_{h_0}(f|_{A_i})$ can be rewritten as

$$\Phi_{h_0}(f) = \sum_{h=h_0}^{\max(H)} \sum_{t} t n_{t,h}. \tag{16}$$

The discrete derivative of the volume of a DEM w.r.t. elevation is hence given by

$$\Phi_{h_0}(f) - \Phi_{h_0+1}(f) = \sum_{t} t n_{t,h_0}. \tag{17}$$

Notice that this expression can be interpreted as the sum of areas of maximally connected subsets of $V^f_{\geq h_0}$ on the slice A_i. In general, when we consider a 2-D domain A of the DEM f, (17) transforms to

$$\Phi_{h_0}(f) - \Phi_{h_0+1}(f) = \sum_{i=n_1}^{n_2} \sum_{t} t n^{(i)}_{t,h_0}. \tag{18}$$

E. Why is a MDGI Considered a Roughness Measure?

In this section, we provide an intuition as to why a MDGI is regarded as a roughness measure. To accomplish this, we consider a special class of DEMs given by

$$\mathcal{F}_{\text{UniPeak}} = \left\{ f : A \to H : \sum_{t} n_{t,h} = 1 \forall\, h \in f(A) \right\} \tag{19}$$

where A denotes a 1-D set, i.e., $\exists m_1 \leq m_2 \in \mathbb{Z}$ such that $A = \{(i_0, j) | m_1 \leq j \leq m_2\}$. It is easy to see that in such a case the set of discrete derivatives given by (17) would effectively be a permutation of the probabilities given by (12). This means that the entropy calculated on the successive discrete derivatives of volume of a DEM is identical to the MDGI when computed on a 1-D uni-peak DEM.

IV. Experiments

In this section, we provide empirical evidence to show that MDGIs capture the characteristic features of a river sub-basin.

A. Study Area and Data Used

We consider lower Indus sub-basin (fluvial), Wardha sub-basin (denudation), and Barmer sub-basin (desert) for the experiments. Catchment basins were first obtained on Shuttle Radar Topography Mission DEM (10 m resolution) using ArcGIS package [6]. The basins are then grouped into watersheds with the help of domain experts. Lower Indus sub-basin, one of the 14 sub-basins lies in between the geographical coordinates of $73°11'$ to $76°44'$ East longitudes and $34°42'$ to $36°9'$ North latitudes, is divided into 31 watersheds of sizes ranging between

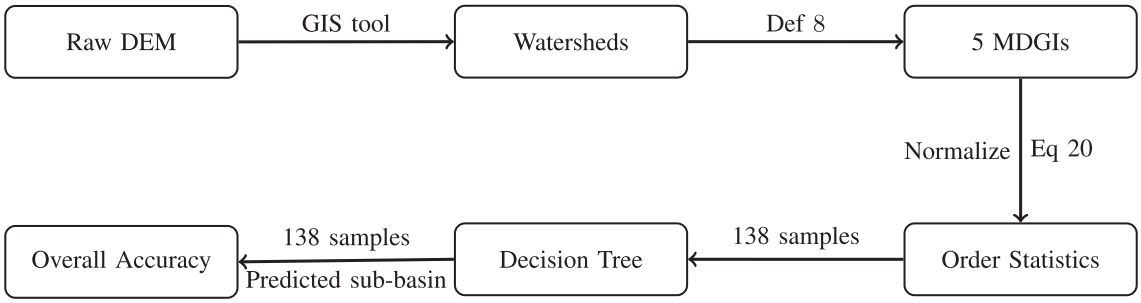

Fig. 10. Schematic diagram illustrating the pipeline of evaluation of the features obtained from MDGIs. The raw cartosat DEM data of each river sub-basin is processed using a standard GIS tool [6] to extract the catchment areas or the watersheds. MDGIs are then computed on each of the watersheds using Def 8 using five structuring elements described in Fig. 2. The MDGIs are then normalized as described in Section IV-C. Order statistics are then constructed using (20). A decision tree of smallest possible depth that can classify three classes, i.e., with depth $= 2$ is then constructed using these features. Overall accuracy of predicted sub-basin type is then used as the evaluation criteria. More details are described in the text.

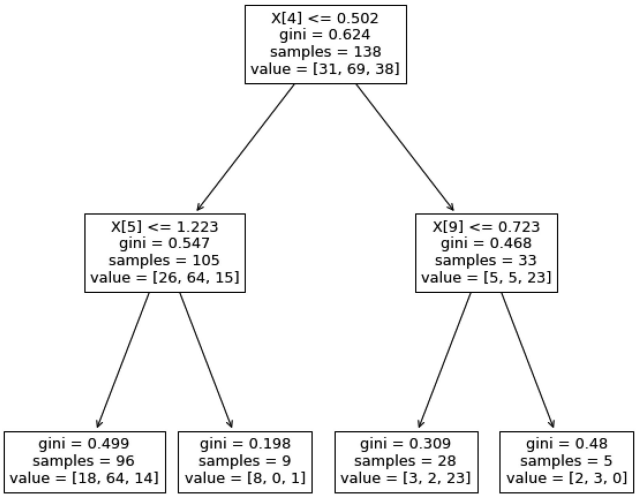

Fig. 11. Decision tree with a depth of 2 is built using the features $X[0], \ldots, X[15]$ based on the MDGIs as described in the text. This decision tree is the smallest possible classification tree that is capable of separating three classes. This classification tree obtains a classification accuracy of $\approx$71% while a random classifier can obtain a maximum classification accuracy of 33.34% on classifying 138 watersheds.

319 sq.km and 1270 sq.km. Wardha sub-basin, one of the principal tributaries of Godavari river, is situated in between the geographical coordinates of $19^\circ 18' N$ and $21^\circ 58' N$ latitudes, and $77^\circ 20' E$ and $79^\circ 45' E$ longitudes. This sub-basin has 69 watersheds. Barmer is another sub-basin of Indus Basin situated between $69^\circ 48'$ and $71^\circ 43'$ East longitudes, and between $25^\circ 28'$ to $27^\circ 69'$ North latitudes. It is fully under Thar Desert and is divided into 38 watersheds. Cartosat DEMs of the Lower Indus sub-basins, Wardha sub-basins, and Barmer sub-basins are illustrated in Fig. 8.

B. Some Preliminary Observations

We compute the MDGIs of all watersheds in each of the river sub-basins using the structuring elements B_1, B_2, B_3, B_4. As there is a variability in the size of each of the watersheds, i.e., the domain of each DEM is of different cardinalities, we normalize these MDGIs with the multiscale granulometric index obtained by using B as the structuring element. As a first observation, for each river, we check the order-statistics of the normalized MDGIs. Fig. 9 shows a plot of the histograms of the maximum and minimum of the normalized MDGIs among the four primary directions across the river sub-basins. These histograms can be viewed as empirical probability distributions. The maximum (respectively minimum) among the normalized MDGIs is denoted as high directional (respectively low directional) in Figs. 8 and 9. It is easy to see that the Barmer sub-basins show a different pattern in the order-statistics as illustrated in Fig. 9. In particular, it is often the case that the maximum is along the direction of B_3 and the lowest is given by B_2, which is not the case with the other two river sub-basins. However, these order-statistics do not help in identifying the differences between Wardha and Lower-Indus sub-basins.

C. More Observations

To identify the differences between the watersheds of all three river sub-basins, we construct features $X[0], \ldots, X[15]$ based on the normalized MDGIs. The details of the construction are as follows:

Let $GI_{B_i}(f)/GI_B(f) = Z_i$ for $i = 1, 2, 3, 4$

$$X[(i-1)4 + (j-1)] = \begin{cases} Z_i & \text{if } Z_{(j)} = Z_i \\ 0 & \text{otherwise} \end{cases} \tag{20}$$

for each $i = 1, 2, 3, 4$ and $j = 1, 2, 3, 4$, where $Z_{(j)}$ denotes the jth order-statistic among Z_1, Z_2, Z_3, Z_4, i.e., $Z_{(1)} \leq Z_{(2)} \leq Z_{(3)} \leq Z_{(4)}$ form a permutation of Z_1, Z_2, Z_3, Z_4. As the number of watersheds (138 altogether) is small, we do not split the data into training and test sets. Instead, we try to obtain interpretable rules that can classify the watersheds into appropriate sub-basins based on the constructed features. A simple decision tree with a depth of 2 is constructed. The depth of the decision tree is restricted so as to ensure that we do not over fit the data. Also, the reason for choosing 2 as the depth is that the minimum depth of a decision tree required to classify 3 classes is 2. We observe that such a decision tree (see Fig. 11) is capable of obtaining $\approx$71% accuracy. Note that a random classifier on the other hand can obtain a maximum accuracy of 33.34%. A schematic diagram summarizing the pipeline of evaluation of the features obtained from MDGIs is provided in Fig. 10.

This experiment indicates that the features computed from MDGIs carry characteristic information of the sub-basins. To explore the discernibility of MDGI-based features, we built decision trees of larger depths until a maximum depth of 9. We observed that the accuracies of decision trees of depths 5, 6, and 9 are ≈86%, ≈89%, and ≈94%, respectively. This indicates that MDGI-based features are useful for river sub-basin classification. However, these features cannot be used as standalone features to classify sub-basins. In order to build better classifiers, one needs to incorporate domain knowledge on the river sub-basins through some form of remotely sensed data or otherwise.

V. Conclusion

In this article, we revisit the roughness measure on DEM data adapted from multiscale granulometries in mathematical morphology, namely MDGI. In earlier works, MDGIs were introduced to capture the characteristic surficial roughness of a river sub-basin along specific directions. They are known to be useful features for classification of river sub-basins. In this article, we provided a theoretical analysis of a MDGI thereby answering the question when such features fail to identify distinct DEMs. In particular, we characterized nontrivial sufficient conditions on the structure of DEMs under which MDGIs are invariant. These properties are illustrated with some fictitious DEMs. We also provided connections to a discrete derivative of volume of a DEM. Based on these connections, we provided intuition as to why a MDGI is considered a roughness measure. Further, we experimentally illustrated on Lower-Indus, Wardha, and Barmer river sub-basins that the proposed features capture the characteristics of the river sub-basin.

Building on the ideas from this article, one can explore at least two directions: 1) building on the main theorem, one can investigate more sufficient conditions ultimately trying to characterize sufficient and necessary conditions on the structure of a DEM such that MDGI is invariant, 2) on the experimental side, use the features proposed in the article alongside other features on river sub-basins to build better classifiers.

Acknowledgment

Kannan Nagajothi would like to thank Regional Remote Sensing Centre, Indian Space Research Organisation. Aditya Challa would like to thank APPCAIR, and Computer Science and Information Systems, BITS-Pilani Goa.

References

[1] J. E. M. Baartman, R. Masselink, S. D. Keesstra, and A. J. A. M. Temme, "Linking landscape morphological complexity and sediment connectivity," *Earth Surf. Processes Landforms*, vol. 38, no. 12, pp. 1457–1471, 2013.

[2] W. Cao *et al.*, "Reunderstanding geomorphological features in chang'e-5 sampling region based on multiscale roughness model," *IEEE J. Sel. Topics Appl. Earth Observ. Remote Sens.*, vol. 14, pp. 9106–9116, Sep. 2021.

[3] L. Chockalingam and B. S. DayaSagar, "Morphometry of network and nonnetwork space of basins," *J. Geophys. Res., Solid Earth*, vol. 110, no. B8, pp. 1–15, 2005, doi: 10.1.29/2005JB003641.

[4] I. V. Florinsky, "Derivation of topographic variables from a digital elevation model given by a spheroidal trapezoidal grid," *Int. J. Geographical Inf. Sci.*, vol. 12, no. 8, pp. 829–852, 1998.

[5] C. H. Grohmann, M. J. Smith, and C. Riccomini, "Multiscale analysis of topographic surface roughness in the Midland Valley, Scotland," *IEEE Trans. Geosci. Remote Sens.*, vol. 49, no. 4, pp. 1200–1213, Aug. 2010.

[6] India Water Resources Information System. Accessed: Jan. 31, 2020. [Online]. Available: https://indiawris.gov.in/wris/#

[7] Y. Kwak, J. Park, and K. Fukami, "Near real-time flood volume estimation from modis time-series imagery in the Indus river basin," *IEEE J. Sel. Topics Appl. Earth Observ. Remote Sens.*, vol. 7, no. 2, pp. 578–586, Oct. 2013.

[8] R. Mantilla and V. K. Gupta, "A GIS numerical framework to study the process basis of scaling statistics in river networks," *IEEE Geosci. Remote Sens. Lett.*, vol. 2, no. 4, pp. 404–408, Oct. 2005.

[9] P. Maragos, "Pattern spectrum and multiscale shape representation," *IEEE Trans.* Pattern Anal. Mach. Intell., vol. 11, no. 7, pp. 701–716, Jul. 1989.

[10] D. C. Mason, D. M. Cobby, M. S. Horritt, and P. D. Bates, "Floodplain friction parameterization in two-dimensional river flood models using vegetation heights derived from airborne scanning laser altimetry," *Hydrol. Processes*, vol. 17, no. 9, pp. 1711–1732, 2003.

[11] J. McKean and J. Roering, "Objective landslide detection and surface morphology mapping using high-resolution airborne laser altimetry," *Geomorphology*, vol. 57, no. 3/4, pp. 331–351, 2004.

[12] V. Morard, P. Dokládal, and E. Decenciere, "One-dimensional openings, granulometries and component trees in $\mathcal{O}(1)$ in per pixel," *IEEE J. Sel. Topics Signal Process.*, vol. 6, no. 7, pp. 840–848, Jan. 2012.

[13] K. Nagajothi and B. S. DayaSagar, "Classification of geophysical basins derived from SRTM and Cartosat DEMS via directional granulometries," *IEEE J. Sel. Topics Appl. Earth Observ. Remote Sens.*, vol. 12, no. 12, pp. 5259–5267, Dec. 2019.

[14] M. Niedda, "Upscaling hydraulic conductivity by means of entropy of terrain curvature representation," *Water Resour. Res.*, vol. 40 no. 4, pp. 1–16, 2004, doi: 10.1029/2003WR002721.

[15] M. Rzadca, "Multivariate granulometry and its application to texture segementation," M.Sc. Thesis, Center for Imaging Science, Rochester Institute of Technology, Rochester, New York, 1994.

[16] B. S. Daya Sagar. *Mathematical Morphology in Geomorphology and GISci*. Boca Raton, FL, USA: CRC Press, 2013.

[17] B. S. Daya Sagar, "Universal scaling laws in surface water bodies and their zones of influence," *Water Resour. Res.*, vol. 43 no. 2, pp. 1–10, 2007, doi: 10.1029/2006WR005075.

[18] B. S. Daya Sagar and L. Chockalingam, "Fractal dimension of non-network space of a catchment basin," *Geophys. Res. Lett.*, vol. 31 no. 12, pp. 1–5, 2004, doi: 10.1029/2004GL019749.

[19] B. S. Daya Sagar and T. L. Tien, "Allometric power-law relationships in a Hortonian fractal digital elevation model," *Geophys. Res. Lett.*, vol. 31, no. 6, pp. 1–4, 2004, doi: 10.1029/2003GL01909.

[20] D. Shen and Y. Sheng, "Area partitioning for channel network extraction using digital elevation models and remote sensing," *IEEE Geosci. Remote Sens. Lett.*, vol. 9, no. 2, pp. 194–198, Sep. 2011.

[21] O. Sizov, "Predictive mapping of glacial and fluvioglacial landforms in the Nadym River Basin (north of west Siberia) with tanDEM-X DEM," *IEEE J. Sel. Topics Appl. Earth Observ. Remote Sens.*, vol. 14, pp. 5656–5666, May 2021.

[22] M. W. Smith, "Roughness in the earth sciences," *Earth- Sci. Rev.*, vol. 136, pp. 202–225, 2014.

[23] L. T. Tay, B. S.Daya Sagar, and H. T. Chuah, "Allometric relationships between traveltime channel networks, convex hulls, and convexity measures," *Water Resour. Res.*, vol. 42 no. 6, pp. 1–9, 2006, doi: 10.1029/2005WR004092.

[24] L. T. Tay, B. S. Daya Sagar, and H. T. Chuah. "Granulometric analyses of basin-wise dems: A comparative study," *Int. J. Remote Sens.*, vol. 28, no. 15, pp. 3363–3378, 2007.

[25] D. L. Turcotte, "Fractals in geology and geophysics," *Pure Appl. Geophys.*, vol. 131, no. 1, pp. 171–196, 1989.

[26] S. C. Tzafestas and P. Maragos, "Shape connectivity: Multiscale analysis and application to generalized granulometries," *J. Math. Imag. Vis.*, vol. 17, no. 2, pp. 109–129, 2002.

[27] S. A. Vardhan, B. S. Daya Sagar, N. Rajesh, and H. M. Rajashekara, "Automatic detection of orientation of mapped units via directional granulometric analysis," *IEEE Geosci. Remote Sens. Lett.*, vol. 10, no. 6, pp. 1449–1453, Jun. 2013.

[28] L. Vincent, "Granulometries and opening trees," *Fundamenta Informaticae*, vol. 41, no. 1/2, pp. 57–90, Jan. 2000.

[29] J. Wen, X. Zhao, Q. Liu, Y. Tang, and B. Dou, "An improved land-surface Albedo algorithm with DEM in rugged terrain," *IEEE Geosci. Remote Sens. Lett.*, vol. 11, no. 4, pp. 883–887, Sep. 2013.

Kannan Nagajothi (Member, IEEE) received the B.Sc. degree in physics from Bharathiar University, Coimbatore, India, in 1986, and the master's degree in computer applications from Indira Gandhi National Open University, New Delhi, India, in 2002.

He is currently a Senior Scientist with the Indian Space Research Organisation, Bangalore, India. He has more than 20 years of work experience in the area of digital image processing, geographical information system, software development, and system management. He has worked on geospatial application projects of national missions and large-scale user projects that involved design and development of large database, system integration, and customized solutions. His research interests include digital image processing, mathematical morphology, GISci and geospatial applications, and decision support systems.

Mr. Nagajothi is a member of GRSS.

Sravan Danda received the B.Math. (Hons.) degree in mathematics from the Indian Statistical Institute, Bangalore, India, in 2009, and the M.Stat. degree in mathematical statistics from the Indian Statistical Institute, Kolkata, India, in 2011, and the Ph.D. degree in computer science from Systems Science and Informatics Unit, Indian Statistical Institute, Bangalore, India, in 2019, under the joint supervision of B. S. Daya Sagar and Laurent Najman.

From 2011 to 2013, he worked as a Business Analyst with Genpact - Retail Analytics, Bangalore, India. He is currently working as an Assistant Professor with the Department of Computer Science and Information Systems, BITS Pilani K K Birla Goa Campus. His current research interests are discrete mathematical morphology and discrete optimization in machine learning.

Aditya Challa received the B.Math. (Hons.) degree in mathematics from the Indian Statistical Institute, Bangalore, India, in 2010, and the master's in complex systems from University of Warwick, Warwick, U.K., in 2012, the Ph.D. degree in computer science from Systems Science and Informatics Unit, Indian Statistical Institute, Bangalore, India, in 2019.

From 2012 to 2014, he worked as a Business Analyst with Tata Consultancy Services, Bangalore, India. From 2019 to 2021, he worked as a Raman PostDoc Fellow with Indian Institute of Science, Bangalore. He is currently working as an Assistant Professor with the Department of Computer Science and Information Systems, BITS Pilani K K Birla Goa Campus. His current research interests focus on using techniques from mathematical morphology in machine learning.

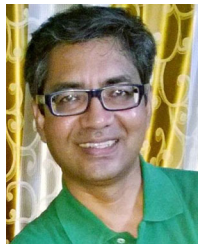

B. S. Daya Sagar (Senior Member, IEEE) received the M.Sc. and Ph.D. degrees in geoengineering and remote sensing from the Faculty of Engineering, Andhra University, Visakhapatnam, India, in 1991 and 1994 respectively.

He is currently a Full Professor of the Systems Science and Informatics Unit (SSIU) with the Indian Statistical Institute, New Delhi, India. He is also the first Head of the SSIU. Earlier, he worked with the College of Engineering, Andhra University, and Centre for Remote Imaging Sensing and Processing (CRISP), The National University of Singapore in various positions during 1992–2001. He was an Associate Professor and Researcher with the Faculty of Engineering & Technology (FET), Multimedia University, Malaysia, during 2001–2007. He has made significant contributions to the field of geosciences, with special emphasis on the development of spatial algorithms meant for geo-pattern retrieval, analysis, reasoning, modeling, and visualization by using concepts of mathematical morphology and fractal geometry. He has authored or coauthored more than 85 papers in journals and has authored and/or guest-edited 11 books and/or special theme issues for journals.

Dr. Daya Sagar recently authored a book entitled *"Mathematical Morphology in Geomorphology and GISci*," CRC Press: Boca Raton, 2013, p. 546. He recently co-edited two special issues on "Filtering and Segmentation with Mathematical Morphology" for IEEE JOURNAL OF SELECTED TOPICS IN SIGNAL PROCESSING (v. 6, no. 7, pp. 737–886, 2012), and "Applied Earth Observation and Remote Sensing in India" for IEEE JOURNAL OF SELECTED TOPICS IN APPLIED EARTH OBSERVATION AND REMOTE SENSING (v. 10, no. 12, p. 5149–5328, 2017). His recent book ''*Handbook of Mathematical Geosciences*," Springer Publishers, p. 942, 2018 reached 750 000 downloads. He was elected as a member of the New York Academy of Sciences in 1995, as a Fellow of the Royal Geographical Society in 2000, as a Senior Member of the IEEE Geoscience and Remote Sensing Society in 2003, as a Fellow of the Indian Geophysical Union in 2011, and as a Fellow of the Indian Academy of Sciences in 2022. He is also a member of the American Geophysical Union since 2004, and a life member of the International Association for Mathematical Geosciences (IAMG). He delivered the "Curzon & Co - Seshachalam Lecture–2009" at Sarada Ranganathan Endowment Lectures (SRELS), Bangalore, and the "Frank Harary Endowment Lecture–2019" at International Conference on Discrete Mathematics–2019 (ICDM–2019). He was awarded the "Dr. Balakrishna Memorial Award" of the Andhra Pradesh Academy of Sciences in 1995, the Krishnan Medal of the Indian Geophysical Union in 2002, the "Georges Matheron Award–2011 with Lectureship" of the IAMG, and the Award of IAMG Certificate of Appreciation–2018. He is the Founding Chairman of the Bangalore Section I EEE GRSS Chapter. He has been recently appointed as an IEEE Geoscience and Remote Sensing Society (GRSS) Distinguished Lecturer (DL) for a two-year period from 2020 to 2022. He is on the Editorial Boards of Computers & Geosciences, Frontiers: Environmental Informatics, and Mathematical Geosciences. He is also the Editor-In-Chief of the Springer Publishers' Encyclopedia of Mathematical Geosciences.